Crystal structure of the biologically active form of class Ib ribonucleotide reductase small subunit from *Mycobacterium tuberculosis*

Malin Uppsten[a], Jamaine Davis[b], Harvey Rubin[b], Ulla Uhlin[a,*]

[a] *Department of Molecular Biology, Swedish University of Agricultural Sciences, Uppsala Biomedical Center, P.O. Box 590, SE-751 24 Uppsala, Sweden*
[b] *Division of Infectious Diseases, Department of Medicine, University of Pennsylvania School of Medicine, Philadelphia, PA 19104, USA*

Received 23 March 2004; revised 12 May 2004; accepted 17 May 2004

Available online 5 June 2004

Edited by Irmgard Sinning

Abstract **Two *nrdF* genes of *Mycobacterium tuberculosis* code for different R2 subunits of the class Ib ribonucleotide reductase (RNR). The proteins are denoted R2F-1 and R2F-2 having 71% sequence identity. The R2F-2 subunit forms the biologically active RNR complex with the catalytic R1E-subunit. We present the structure of the reduced R2F-2 subunit to 2.2 Å resolution. Comparison of the R2F-2 structure with a model of R2F-1 suggests that the important differences are located at the C-terminus. We found that within class Ib, the E-helix close to the iron diiron centre has two preferred conformations, which cannot be explained by the redox-state of the diiron centre. In the R2F-2 structure, we also could see a mobility of αE in between the two conformations.**
© 2004 Federation of European Biochemical Societies. Published by Elsevier B.V. All rights reserved.

Keywords: Crystal structure; Ribonucleotide reductase; R2; Diiron carboxylate protein; Tyrosyl radical; *Mycobacterium tuberculosis*

1. Introduction

Ribonucleotide reductase catalyses the reduction of all four ribonucleotides to their corresponding deoxyribonucleotides and therefore plays a central role in DNA biosynthesis and nucleotide metabolism. Three distinctly different classes of ribonucleotide reductase (RNR) have been described [1–4], which share the common feature of the radical-based catalytic mechanism [5,6]. Several organisms have been found to code for two or even three classes of RNR [7,8].

All mammalian RNRs, as well as that from aerobically grown *Escherichia coli*, and DNA viruses belong to class I and use non-heme binuclear iron cofactors for generation of the essential tyrosyl radicals [9,10]. Class I enzymes have further been divided into Ia and Ib after the discovery of a new type of RNR with a new pattern of allosteric activity regulation [7]. The class Ia enzymes have two different allosteric binding sites, one site where binding of ATP activates and dATP inhibits nucleotide reduction (the on/off switch) and one binding site for substrate specificity [11,12]. The on/off switch is missing in class Ib [7,13].

All class I enzymes are composed of two homodimeric proteins, R1 and R2. To distinguish between subclass Ia and Ib the proteins of class Ib RNRs are named R1E and R2F after their encoding genes *nrdE* and *nrdF*, respectively [14]. Binding sites for substrates (NDPs) and allosteric effectors (ATP, dNTPs) are localised in the large R1 subunit [15]. The small R2 subunit contains a tyrosyl free radical that is produced by a neighbouring diiron site. Since the discovery of the stable tyrosyl radical [16] in RNR from *E. coli* (class Ia), this enzyme has been extensively studied. Based on structural and biochemical studies, a long-range coupled electron/proton transfer over 35 Å [17–20] and a substrate–radical catalytic mechanism [21] have been established.

The class Ib RNRs have been found in widely different prokaryotes, including *Salmonella typhimurium*, *Lactococcus lactis*, *Bacillus subtilis*, *Mycoplasma genitalium*, and *Mycobacterium tuberculosis* (Mtb), as well as in aerobically grown *E. coli* [14,22–25]. In the cases known, class Ib RNRs are normally not expressed in vivo, with the only exception so far being Mtb RNR. The RNR enzyme from this pathogen has attracted attention because tuberculosis remains a major global disease infecting one-third of the world population and killing more than 2 million people each year [26]. The resistance against known drugs is becoming an increasing problem and since RNR is a potential drug target it is important to investigate the features of this particular enzyme.

The class Ib R1E homo-dimer from Mtb has a predicted molecular mass of 2×83 kDa. Surprisingly, two separate genes, *nrdF1* and *nrdF2*, encode for the small RNR protein. They are denoted R2F-1 and R2F-2 and have 71% amino acid identity [27]. The calculated molar masses of R2F-1 and R2F-2 are 2×36.6 kDa (322 amino acids per monomer) and 2×37.0 kDa (324 amino acids per monomer), respectively. Both are postulated to contain an iron-radical site like other class I R2 proteins [27]. Enzymatic investigations revealed that R2F-2 forms the recombinant active enzyme together with R1E. Also R2F-1 was able to form a holo-complex with R1E in vivo, but only if it was present in concentrations higher than the R2F-2. It was suggested that there might be a second R1E to complement R2F-1 or that an active complex with the known R1E forms when R2F-1 is present in high enough concentrations.

The C-terminus of the small subunit is shown to be essential for binding to the large subunit for formation of the holo-complex [28–30]. This binding is species specific and can thus be used for constructing drugs to prevent the formation of

* Corresponding author. Fax: +46-18-536971.
E-mail address: ulla.uhlin@molbio.slu.se (U. Uhlin).

Abbreviations: RNR, ribonucleotide reductase; Mtb, *Mycobacterium tuberculosis*; EPR, electron paramagnetic resonance

0014-5793/$22.00 © 2004 Federation of European Biochemical Societies. Published by Elsevier B.V. All rights reserved.
doi:10.1016/j.febslet.2004.05.059

RNR holo-complexes in pathogens. The binding pocket for the R2 C-terminus on R1 has been identified in *E. coli* [19] but no structure of any RNR class I holo-complex has yet been published. Of the class I RNRs, crystal structures of R1 and R2 subunits from *E. coli* and R1E and R2F from *S. typhimurium* have been solved, as well as the R2 protein from mouse, the R2/R4 protein from *S. cerevisiae* and R2F from *C. ammoniagenes* [4].

Here, we present the structure of the class Ib small subunit R2F-2 from Mtb with the diiron site in its reduced state. The structure shows a similar fold to the previously solved structures of class Ib R2F subunits from *S. typhimurium* [31] and *C. ammoniagenes* [32].

2. Materials and methods

2.1. Overexpression and purification

The overexpression and purification of the R2F-2 protein from Mtb was performed as described earlier [27].

2.2. Crystallisation

The protein was crystallised using the hanging drop vapour diffusion method. Initial crystals were obtained in Hampton Screen II, tube no. 14 diluted 1:1 with distilled water. The drops with the refined crystallisation condition contained a 1:1 mix of protein solution (22 mg/ml R2F-2 in 50 mM Tris, pH 7.5, 0.1 mM DTT) and reservoir solution consisting of 0.6 M ammonium sulfate, 100 mM sodium citrate buffer, pH 5.6, and 50 mM Na/K tartrate. Crystals in the shape of rhombohedral plates started growing at 15 °C after 1 day and increased in size for approximately 1 week.

2.3. Data collection and refinement

Crystals were cryo protected using reservoir solution supplemented with 30% glycerol and immediately flash-cooled in liquid nitrogen.

Diffraction data were collected at the European Synchrotron Radiation Facility (ESRF), beamline ID29, Grenoble, France. The HKL software suite programs [33] were used for data processing and scaling. For initial phasing, molecular replacement was performed in the program Molrep (ccp4) [34,35] using the R2F structure of *S. typhimurium* RNR as search model. This structure was also used to create a model of Mtb R2F-2 with the program Swiss Model [36]. The resulting model became the starting structure for rebuilding. After rigid body refinement and subsequent maximum likelihood refinement (Refmac5, ccp4 suite) [37], water picking was performed with wARP (ccp4) [38].

The crystals belong to the tetragonal spacegroup $P4_22_12$ and the cell parameters are $a = b = 161$ Å, $c = 116$ Å. There are three subunits in the asymmetric unit, one dimer and one single monomer making up for a solvent content of 63%. A threefold NCS constraint was used in the beginning of the refinement to ease model building, but as the refinement proceeded differences between the molecules arose and the restraint was removed.

The free *R*-value was calculated from 5% of the data and monitored throughout the refinement. Interpretation of maps and model building were performed using the program O [39]. Stereochemical quality was evaluated with Procheck [40] and analysis of the agreement between the atomic model and X-ray data was performed with Sfcheck [41] and EDS [42]. Data and refinement statistics are summarised in Table 1.

Initial coordinates, topology and parameter files for the small molecules found in the structure (citrate and glycerol) were taken from the HIC-UP ligand database [43].

Table 1
Data collection and refinement statistics

Beamline	ESRF, ID29
Wavelength (Å)	0.9756
Cell parameters (Å, °)	161, 161, 116, 90, 90, 90
Space group	$p4_22_12$
Resolution range (Å)	40–2.2 (2.24–2.20)
Redundancy	4.84
R_{merge} [a]	9.1 (44.4)
I/σ (I)	10.0 (1.7)
Completeness (%)	99.0 (93.5)
No. observations	373,499
No. unique reflections	77,125
R_{cryst} [b]	0.18
R_{free} [c]	0.20
No. non-hydrogen atoms	7359
No. solvent molecules	391
r.m.s.d. bond length (Å)	0.023
r.m.s.d. angle (°)	1.85
Average *B*-factor (Å^2)	28.4

Numbers in parentheses refer to the highest resolution shell.
[a] $R_{merge} = (\sum_{hkl}\sum_i |I_i(hkl) - \langle I(hkl)\rangle| / \sum_{hkl}\sum_i I_i(hkl)) \times 100\%$ for n independent reflections and i observations of a given reflection. $\langle I(hkl)\rangle$ is the average intensity of the I observation.
[b] $R_{cryst} = \sum_h ||F_o(h)| - |F_c(h)|| / \sum_h |F_o(h)|$, where F_o and F_c are the observed and calculated structure factors, respectively.
[c] R_{free} is equivalent to F_{cryst} for a 5% subset of reflections not used in the refinement.

3. Results and discussion

3.1. Overall structure

The R2F-2 from Mtb is an all helical protein and has a similar fold to the former known R2 structures [18,31,32,44]. As expected, it is most similar to the structures of *S. typhimurium* R2F (rmsd 1.04 Å for 283Cα) and *C. ammoniagenes* R2F (rmsd 0.86 Å for 285Cα). These class Ib RNRs have a sequence identity of 77% and 66%, respectively, to Mtb R2F-2.

One R2F-2 monomer is made up of 11 helices of which eight, αA-H, form a bundle. Three shorter helices, α1, α2 and α4, are peripherally located in the structure (Fig. 1). There are three monomers in the asymmetric unit, one dimer and one monomer creating a dimer interaction through a crystallographic twofold axis. The shape of the R2 dimer from *E. coli* has been compared to a heart where each monomer forms one lobe and two β-strands form the tip of the heart. The two β-strands are missing in all other solved R2 structures including the Mtb R2F-2.

The electron density is well defined for all three subunits. Of the 324 amino acids in the R2F-2 sequence, 288 have been traced in the electron density for the best defined subunit. The first 8–9 residues are not visible as well as the last 28–38 residues, with variations between the molecules in the asymmetric

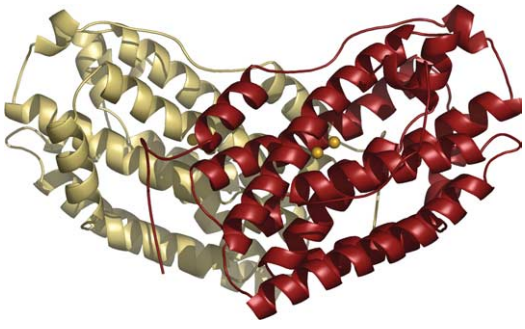

Fig. 1. Structure of *Mycobacterium tuberculosis* R2F-2 dimer. The subunits are coloured in beige and red, respectively, and the irons in the metal centre are shown as yellow spheres. Figs. 1, 2 and 4 were prepared using PyMOL [55].

unit. The extra N-terminal helix in *C. ammoniagenes*, named α0, is not present in Mtb R2F-2.

The unstructured C-terminus seems to be a common feature of all R2 structures and it is thought to facilitate the interaction with the larger subunit. Studies performed with NMR have shown that the C-terminal peptide of R2 becomes structured upon binding to R1 [45,46] and several enzymatic experiments show that the C-terminus of R2 is an effective inhibitor for complex formation between R1 and R2 [27–29,47,48].

During the refinement it became apparent from the electron density maps that amino acid residue 146 probably is a serine and not a tyrosine as sequenced. There is not enough room for the side chain of a tyrosine (Fig. 2).

3.2. The metal site

The crystals were not treated with any reducing agent prior to data collection and were probably in their oxidised state when subjected to X-ray radiation. However, the coordination of the irons in Mtb R2F-2 is characteristic for a reduced iron centre (Fig. 3(a) and (b)).

The two irons in R2F-2 are ligated by two histidines (His106, His200), one aspartate (Asp72), three glutamates (Glu103, Glu163, Glu197) and one water molecule. Glutamate 103 and 197 are both bridging the two irons, and Glu163 ligates bidentate to Fe2. The water molecule binds only to Fe2 making it six-coordinate with a square-pyramidal shape as opposed to Fe1, which has four ligands creating a tetrahedral coordination. This coordination is identical in the structure of the reduced *S. typhimurium* R2F, while in the reduced *C. ammoniagenes* R2F, the water molecule ligating Fe2 is absent. In the structure of the reduced *E. coli* R2, there is no water coordinating any of the irons and the glutamate corresponding to Glu163 ligates monodentate to Fe2, not bidentate as in the class Ib enzymes. Where both the ferrous and the ferric states of the iron site have been studied from the same class Ib R2F, this glutamate changes its conformation between the states. The glutamate moves from bidentate binding of the Fe2 in the ferrous state to monodentate binding in the ferric state. By this move, space is formed for one of the bridging glutamates, which then in the oxidised state loses the ligand to Fe1 and only ligates Fe2 (Fig. 3(b) and (c)).

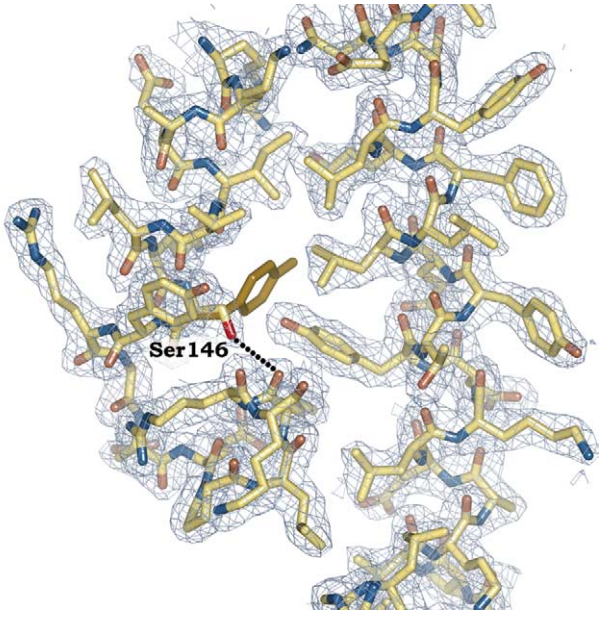

Fig. 2. The helices D, E (left) and G (right) in R2F-2. During the structure refinement, it became apparent from the electron density maps that residue 146 in the C-terminal part of αD is a serine and not a tyrosine as earlier sequenced. The serine makes a clear hydrogen bond to the carbonyl oxygen of residue 154 in the N-terminal part of αE. The final $2F_o–F_c$ map is contoured at 1σ and the tyrosine side chain is shown in khaki.

The intermetal distances in R2F-2 from Mtb are between 3.5 and 3.7 Å varying slightly among the different molecules in the asymmetric unit. The corresponding distances in the reduced *C. ammoniagenes* and *S. typhimurium* R2F structures are 3.9 and 3.7 Å, respectively. In the reduced *E. coli* R2 structure, the iron–iron distance is 3.9 Å.

The predominantly seen reduced iron centre is thought to be an effect of reduction in the X-ray beam. Glu197 in Mtb is not perfectly defined in the electron density maps, suggesting a non-uniform conformation possibly indicating slightly different oxidation states between the molecules in the crystal. A similar reducing effect was observed in the *S. typhimurium* and *C. ammoniagenes* structures [31,32] as well as in thawed and refrozen R2 protein from *E. coli* [49]. Reduction by X-ray radiation has also been reported for other diiron enzymes [50].

Several datasets were collected, but all of them were found to be reduced. Combination of initial images from different crystals shows only minor differences compared to full datasets. When the structure of R2F from *S. typhimurium* was solved, it was discovered that the use of glycerol as a cryo protectant promoted reduction of the diiron centre, and to capture the oxidised state PEG400 was used. In the case of Mtb R2F-2, however, the metal centre was found to be reduced with either glycerol or PEG400 as cryo protectant.

A theoretical model of the oxidised iron centre in R2F-2 from Mtb was made based on the *S. typhimurium* structure [51]. The arrangement of the carboxylate ligands in the model of the oxidised Mtb protein is identical to the one seen in the X-ray structure of R2F-2 with a reduced metal centre. According to the theoretical model, the only differences between the two states might be the ligation of water molecules and the presumed μ-oxo bridge in the oxidised state. If this model is correct, assuming only minor differences between the states, it might be difficult to distinguish the oxidised from the reduced state.

3.3. The tyrosyl radical

The radical forming tyrosine in Mtb R2F-2, Tyr110, is about 6.8 Å from the closest iron atom. The corresponding distances in *C. ammoniagenes* and *S. typhimurium* are 7 and 6.5–7 Å, respectively. In *E. coli* R2, the position of the tyrosine responsible for storing the radical differs from the position in the class Ib proteins. Tyr122 in *E. coli* R2 is situated about 5 Å from Fe1, whereas in the class Ib structures solved so far this distance is longer and bridged by a water molecule. The more distant tyrosine and the bridging water molecule have been suggested to be common features among the class Ib proteins [32]. The long iron-radical distance in Mtb has previously been indicated by EPR measurements. It was found that saturation of the tyrosyl radical occurs at lower applied microwave power than that of the tyrosyl radicals in *E. coli* and mouse [51,52] reflecting a much weaker magnetic interaction between the radical and the iron centre and thus also a longer distance

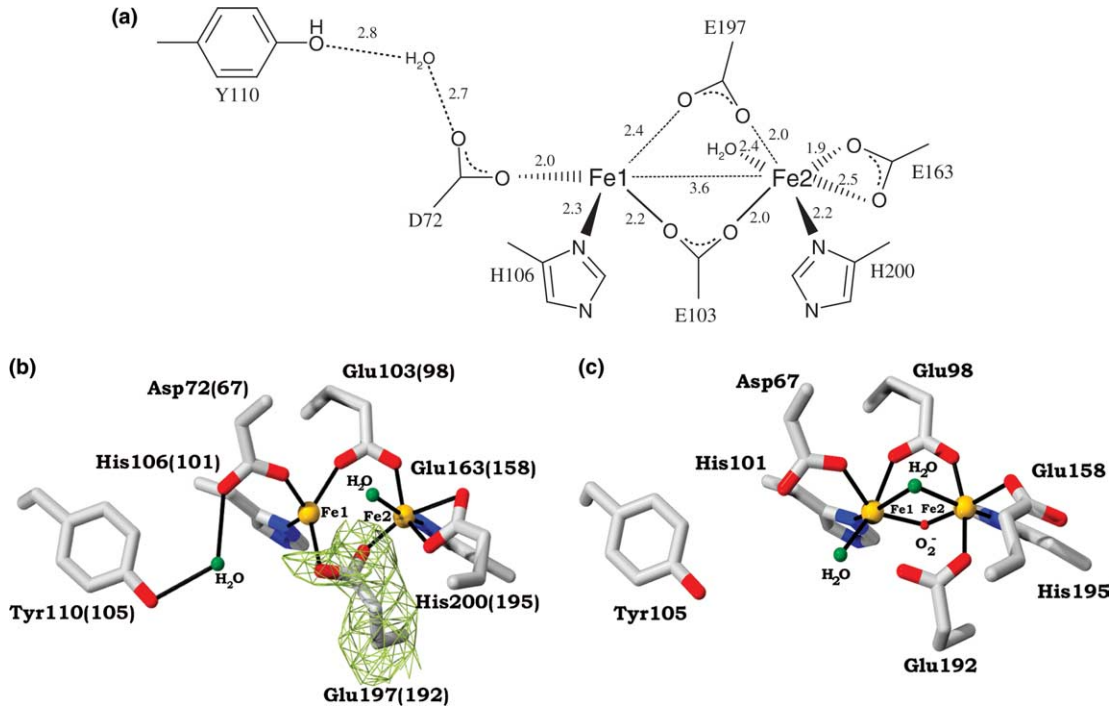

Fig. 3. Comparison of reduced and oxidised diiron centres. (a) Schematic picture of the reduced diiron site in Mtb R2F-2. (b) Crystallographic structure of the reduced diiron site in R2F-2 from Mtb. The iron coordination is identical to the one in the reduced *S. typhimurium* R2F (numbering in parenthesis). Final F_o–F_c map is contoured at 3σ where the iron ligating Glu197 was excluded from the calculation. (c) Structure of the oxidised diiron centre in *S. typhimurium*. (a) was made using MDL®ISIS/Draw. (b) and (c) were made using Swiss-Pdb Viewer [56] (official URL, http://expasy.org/spdbv) and rendered with POV-Ray (official URL, http://www.povray.org).

between them. This is consistent with the structural differences described above.

The iron centre in Mtb R2F-2 was studied at high EPR microwave frequency at 4 K reporting a high g1, indicating a predominantly non-hydrogen bonded tyrosyl radical [53,51,54]. In the crystal structure of the reduced R2F-2 from Mtb, Tyr110 is in its protonated state and within hydrogen bonding distance (2.8 Å) of a water molecule, which in turn forms a hydrogen bond to Asp72. The distance between the phenolic oxygen of Tyr110 and the closest carboxylate oxygen of Asp72 is 4.5–4.8 Å. The radical site in the R2F protein from *S. typhimurium* has similar features in its reduced state, with a water molecule forming a bridge between the tyrosine and the iron-ligating aspartate. When the structure of *S. typhimurium* R2F was solved with an oxidised radical site, however, the presence of the water molecule could not be assured, leaving the tyrosine without hydrogen bonds closer than 4 Å away from the aspartate. Crystallographic investigations of *C. ammoniagenes* show that the water molecule is present in both oxidation states, hydrogen bonding to the tyrosine residue.

EPR measurements have further characterised the structure of the tyrosyl radical in Mtb R2F-2, indicating the β-methylene protons of the tyrosine side chain to be situated with dihedral angles of about 50° (θ_1) and 70° (θ_2) with respect to the p_z orbital of the aromatic ring [51]. These values differ somewhat from the ones observed in the X-ray structure, where θ_1 varies between 38° and 43°, and θ_2 between 77° and 82° in the three molecules in the asymmetric unit.

The tyrosine residue involved in radical storage in RNR is in all known structures located in a hydrophobic pocket close to the metal centre. By EPR studies, the tyrosine in Mtb R2F-2 is shown to have the same locked conformation at all temperatures, suggesting a rigid environment [51]. This unusual stability is, however, not possible to explain by structural comparisons to other R2 proteins.

3.4. The αE helix

The αE is one of the helices in the four-helix bundle providing ligands to the metal centre. In all solved R2 structures, the hydrogen-bonding pattern of the αE helix is distorted. This is due to an extra amino acid causing the formation of a π-type turn in the middle of the helix.

The distortion differs among earlier determined R2 structures [31,32,44,49] and there seems to be a tendency for two conformations of αE among the class Ib structures (Fig. 4). One of the preferred conformations (conf 1) is seen in the structure of Mtb R2F-2, where the diiron centre is reduced. It has the same conformation as αE in *S. typhimurium* when the diiron centre is oxidised (rmsd 0.24 for 29 Cα atoms in αE). In the structure of *S. typhimurium* where the irons are reduced, however, the conformation of αE (conf 2) is very similar to the one seen in the structures of *C. ammoniagenes* regardless of the redox-state of the metal centre.

Variations between the conformations are most distinct in one helix turn between two conserved phenylalanines (Phe167 and Phe171 in Mtb) and the most pronounced movement is displayed by a tyrosine residue (Tyr168 in Mtb, Tyr163 in *S. typhimurium*). The position of the tyrosine differs by about 2.5 Å between the two conformations. In Mtb R2F-2, conf 1, the tyrosine stretches out to the surface of the protein and in the oxidised structure of *S. typhimurium* the corresponding Tyr163 forms a hydrogen bond to residue 288 stabilising a few addi-

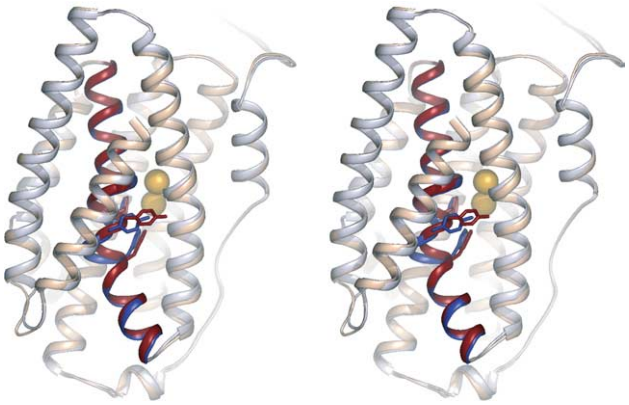

Fig. 4. Stereo cartoon showing conformational differences in helix E. Comparison of the Mtb R2F-2 monomer with the R2F monomer from *S. typhimurium*, both with reduced Fe-centre. The Mtb R2F-2 monomer is coloured in pink and its helix E in red, whereas R2F from *S. typhimurium* is shown in light blue and its helix E in darker blue. The two monomers have very similar folds except in the helix E region where the most pronounced movement is displayed by a tyrosine (Y168 in Mtb, Y163 in *S. typhimurium*). The tyrosine residue stretches out to the surface of the protein in the Mtb structure. The two iron ions are shown as yellow spheres.

tional amino acids in the C-terminal part of the structure. This hydrogen bond, however, can not be observed in the Mtb structure.

Differences seen between the two preferred conformations are very similar to those observed between the reduced wt *E. coli* R2 and a mutant where Ser211 was mutated to an alanine [49]. With the exception of R2F from *S. typhimurium*, there is no correlation between alternate conformations of αE and the redox-state of the diiron centre in wild type R2 proteins of either class Ia or Ib.

In the Mtb R2F-2 structure, there are indications of movements in the αE helix. Difference Fourier maps (Fo-Fc) reveal that αE has more than one conformation, indicating mobility from conf 1 towards conf 2. The movement of αE, however, can not be associated with a certain redox-state of the metal centre and the mobility of the helix has not been possible to explain by data currently available. However, there is a possibility that it could be an effect of radiation.

3.5. R2F-1

A three-dimensional molecular model for Mtb protein R2F-1 was built based on the structure of Mtb R2F-2. The proteins are homologous, having a 71% identity on the amino acid level. All the iron ligands and mechanism-related residues are conserved in both proteins as well as the residues postulated to be involved in the hydrogen bonded pathway for the radical. The hydrophobic pocket where the tyrosyl radical is stored is almost identical in the two proteins. The only difference is Met189 in R2F-2, which is a leucine in R2F-1. This hydrophobic residue is located about 7 Å from the radical storing tyrosine and is by this exchange unlikely to affect the stability of the radical. The R2F from *S. typhimurium* also has a leucine at this position, while in *C. ammoniagenes* there is an isoleucine.

A comparison of the αE region in the R2F-2 structure and the R2F-1 model reveals very similar structures. The biggest difference is a phenylalanine in R2F-2 (Phe258), which is a tyrosine in R2F-1. This residue is positioned on αH, adjacent to αE, in the gate where the most prominent movement of αE takes place. A tyrosine at this position could enable stabilisation of the αE helix by the formation of a hydrogen bond between the hydroxyl group of the tyrosine and the carbonyl oxygen of residue 168 (R2F-2 numbering) in αE. In all R2F subunits known so far, this residue is a phenylalanine except for R2F-1 from Mtb where it is a tyrosine. Also, the class Ia R2 proteins, *E. coli* and mouse, have tyrosines at this position but the hydrogen bond suggested above cannot be observed in the X-ray structures of these proteins.

The structural similarity between R2F-1 and R2F-2 indicates that both should be functional for radical transfer. So, why does not R2F-1 function together with R1E? The answer can probably be found in the differences in amino acid composition of the C-terminus of the two R2Fs. Inhibition studies with C-terminal peptides illustrate that the R1E protein has a much higher affinity for the C-terminus of R2F-2 than that of R2F-1 [27]. These results, in combination with enzymatic studies, demonstrate that R2F-2 is more likely to be the complementing subunit to R1E, able to form an active holo-complex. The true function of R2F-1 requires further elucidation.

The coordinates and structure factors have been deposited at the PDB databank: code 1uzr (coordinates) and code r1uzrsf (structure factors).

Acknowledgements: This work was supported by the Strategic Nucleic Acid Research Program, Swedish Research Foundation and Swedish Cancer Foundation. We thank ESRF for beamtime and for help with data collection. We thank Prof. Hans Eklund for fruitful discussions concerning the structure and Mark Harris for corrections of the manuscript.

References

[1] Reichard, P. (1993) Science 260, 1773–1777.
[2] Stubbe, J. (1990) J. Biol. Chem. 265, 5329–5332.
[3] Sjöberg, B.M. (1997) Struct. Bonding 88, 139–173.
[4] Eklund, H., Uhlin, U., Färnegårdh, M., Logan, D.T. and Nordlund, P. (2001) Prog. Biophys. Mol. Biol. 77, 177–268.
[5] Gräslund, A. and Sahlin, M. (1996) Annu. Rev. Biophys. Biomol. Struct. 25, 259–286.
[6] Stubbe, J. and van der Donk, W.A. (1998) Chem. Rev. 98, 705–762.
[7] Eliasson, R., Pontis, E., Jordan, A. and Reichard, P. (1996) J. Biol. Chem. 271, 26582–26587.
[8] Dawes, S.S., Warner, D.F., Tsenova, L., Timm, J., McKinney, J.D., Kaplan, G., Rubin, H. and Mizrahi, V. (2003) Infect. Immun. 71, 6124–6131.
[9] Gräslund, A., Sahlin, M. and Sjöberg, B.M. (1985) Environ. Health Perspect. 64, 139–149.
[10] Larsson, A. and Sjöberg, B.M. (1986) EMBO J. 5, 2037–2040.
[11] Thelander, L. and Reichard, P. (1979) Annu. Rev. Biochem. 48, 133–158.
[12] Eriksson, M. (1997) in: Department of Molecular Biology Swedish University of Agricultural Sciences, Uppsala.
[13] Uppsten, M., Färnegårdh, M., Jordan, A., Eliasson, R., Eklund, H. and Uhlin, U. (2003) J. Mol. Biol. 330, 87–97.
[14] Jordan, A., Gibert, I. and Barbe, J. (1994) J. Bacteriol. 176, 3420–3427.
[15] von Döbeln, U. and Reichard, P. (1976) J. Biol. Chem. 251, 3616–3622.
[16] Ehrenberg, A. and Reichard, P. (1972) J. Biol. Chem. 247, 3485–3488.
[17] Climent, I., Sjöberg, B.M. and Huang, C.Y. (1992) Biochemistry 31, 4801–4807.

[18] Nordlund, P., Sjöberg, B.M. and Eklund, H. (1990) Nature 345, 593–598.
[19] Uhlin, U. and Eklund, H. (1994) Nature 370, 533–539.
[20] Siegbahn, P.E.M., Blomberg, M.R.A. and Crabtree, R.H. (1997) Theor. Chem. Acc. 97, 289–300.
[21] Mao, S.S., Holler, T.P., Yu, G.X., Bollinger Jr., J.M., Booker, S., Johnston, M.I. and Stubbe, J. (1992) Biochemistry 31, 9733–9743.
[22] Jordan, A., Pontis, E., Åslund, F., Hellman, U., Gibert, I. and Reichard, P. (1996) J. Biol. Chem. 271, 8779–8785.
[23] Scotti, C., Valbuzzi, A., Perego, M., Galizzi, A. and Albertini, A.M. (1996) Microbiology (UK) 142, 2995–3004.
[24] Fraser, C.M., Gocayne, J.D., White, O., Adams, M.D., Clayton, R.A., Fleischmann, R.D., Bult, C.J., Kerlavagne, A.R., Sutton, G., Kelley, J.M., Fritchman, J.L., Weidman, J.F., Small, K.V., Sandusky, M., Fuhrmann, J., Nguyen, D., Utterback, T.R., Saudek, D.M. and Venter, J.C. (1995) Science 270, 397–403.
[25] Yang, F.D., Lu, G.Z. and Rubin, H. (1994) J. Bacteriol. 176, 6738–6743.
[26] WHO (2003) Geneva.
[27] Yang, F.D. et al. (1997) J. Bacteriol. 179, 6408–6415.
[28] Cohen, E.A., Gaudreau, P., Brazeau, P. and Langlier, Y. (1986) Nature 321, 441–442.
[29] Dutia, B.M., Frame, M.C., Subak-Sharpe, J.H., Clark, W.N. and Marsden, H.S. (1986) Nature 321, 439–441.
[30] Cosentino, G. et al. (1991) Biochem. Cell Biol. 69, 79–83.
[31] Eriksson, M., Jordan, A. and Eklund, H. (1998) Biochemistry 37, 13359–13369.
[32] Högbom, M., Huque, Y., Sjöberg, B.M. and Nordlund, P. (2002) Biochemistry 41, 1381–1389.
[33] Otwinowski, Z. and Minor, W. (1997) Methods Enzymol. 276, 307–326.
[34] Vagin, A. and Teplyakov, A. (1997) J. Appl. Cryst. 30, 1022–1025.
[35] Collabororative Computational Project No. 4 (1994) Acta Crystallogr. D 50, 760–763.
[36] Schwede, T., Kopp, J., Guex, N. and Peitsch, M.C. (2003) Nucleic Acids Res. 31, 3381–3385.
[37] Murshudov, G.N., Vagin, A.A. and Dodson, E.J. (1997) Acta Crystallogr., Sect. D 53, 240–255.
[38] Perrakis, A., Sixma, T.K., Wilson, K.S. and Lamzin, V.S. (1997) Acta Crystallogr., Sect. D 53, 448–455.
[39] Jones, T.A., Zou, J.Y., Cowan, S.W. and Kjeldgaard, M. (1991) Acta Crystallogr. 47, 110–119.
[40] Laskowski, R.A., Macarthur, M.W., Moss, D.S. and Thornton, J.M. (1993) J. Appl. Crystallogr. 26, 283–291.
[41] Vaguine, A.A., Richelle, J. and Wodak, S.J. (1999) Acta Crystallogr., Sect. D 55, 191–205.
[42] Kleywegt, G.J., Harris, M.R., Zou, J.Y., Taylor, T.C., Wählby, A. and Jones, T.A. (2003) The Uppsala Electron Density Server, accepted (Acta Cryst. D/CCP4 Proceedings).
[43] Kleywegt, G.J. and Jones, T.A. (1998) Acta Crystallogr., Sect. D 54, 1119–1131.
[44] Kauppi, B., Nielsen, B.B., Ramaswamy, S., Larsen, I.K., Thelander, M., Thelander, L. and Eklund, H. (1996) J. Mol. Biol. 262, 706–720.
[45] Lycksell, P.O., Ingemarson, R., Davis, R., Gräslund, A. and Thelander, L. (1994) Biochemistry 33, 2838–2842.
[46] Lycksell, P.O. and Sahlin, M. (1995) FEBS Lett. 368, 441–444.
[47] Yang, F.D., Spanevello, R.A., Celiker, I., Hirschmann, R., Rubin, H. and Cooperman, B.S. (1990) FEBS Lett. 272, 61–64.
[48] Climent, I., Sjöberg, B.M. and Huang, C.Y. (1991) Biochemistry 30, 5164–5171.
[49] Logan, D.T., Su, X.D., Åberg, A., Regnström, K., Hajdu, J., Eklund, H. and Nordlund, P. (1996) Structure 4, 1053–1064.
[50] Lindqvist, Y., Huang, W.J., Schneider, G. and Shanklin, J. (1996) EMBO J. 15, 4081–4092.
[51] Liu, A., Potsch, S., Davydov, A., Barra, A.L., Rubin, H. and Gräslund, A. (1998) Biochemistry 37, 16369–16377.
[52] Elleingand, E. et al. (1998) Eur. J. Biochem. 258, 485–490.
[53] Liu, A.M., Barra, A.L., Rubin, H., Lu, G.Z. and Gräslund, A. (2000) J. Am. Chem. Soc. 122, 1974–1978.
[54] Liu, A. and Gräslund, A. (2000) J. Biol. Chem. 275, 12367–12373.
[55] DeLano, W.L. (2002) DeLano Scientific, San Carlos.
[56] Guex, N. and Peitsch, M.C. (1997) Electrophoresis 18, 2714–2723.